RSC Advances

ROYAL SOCIETY OF CHEMISTRY

www.rsc.org/advances

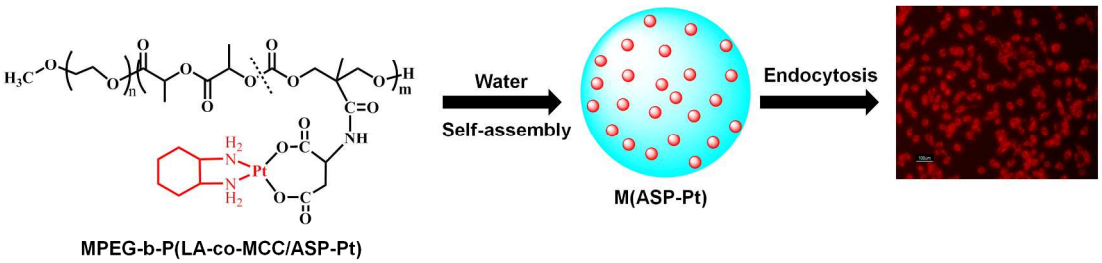

MPEG-b-P(LA-co-MCC/ASP-Pt)

Biodegradable polymers with pendent pair-wised carboxylic acids but lacking sulfur were used to chelate oxaliplatin prodrug which self-assembled into micelles in water for drug delivery.

Journal Name

ARTICLE

Biodegradable polymer-platinum drug conjugates to overcome platinum drug resistance

Received 00th January 20xx,
Accepted 00th January 20xx

DOI: 10.1039/x0xx00000x

www.rsc.org/

Qiang Yang,[†a] Ruogu Qi,[†b] Jing Cai,[a] Xiang Kang,[a] Si Sun,[a] HaihuaXiao,[b] XiabinJing,[b] Wenliang Li,[*c] and Zehua Wang[*a]

Drug resistance and severe dose-dependent side effects are the major obstacles to the further use of the platinum agents. Two well-acknowledged mechanisms of resistance are the decreased intracellular accumulation and the increased sulfur-binding-detoxification of platinum agents. The polymer-drug conjugate approach can remarkably enhance the uptake of substances by cancer cells, therefore can achieve better anticancer effects with lower dosage, thus reduce the dose-dependent side effects. Here we synthesized a biodegradable polymer containing pendant 1,2-bidentate carboxyl groups to chelate platinum without introducing sulfur atoms to potentially detoxify the platinum drugs. The polymer-platinum conjugates formed nanomicelles showed significantly increased intracellular accumulation and could partially overcome drug resistance in ovarian cancer cells.

1 Introduction

Oxaliplatin as the third generation of platinum(II)-based drugs, has been widely used in clinic practice.[1, 2] The study on the of platinum(II) drugs has indicated that 1,2-cyclohexanediamine works as a stable ligand of Pt atom while the oxalic acid is a leaving ligand in the oxaliplatin molecule.[3, 4] The hydrolysis of oxaliplatin in the cancer cells would result in the formation of the active anticancer species of [(1R,2R)-1,2-diaminocyclohexane] platinum(II) (DACH-Pt), which forms 1,2-(GpG) crosslinks with DNA to inhibit its replicating.[4-7] In this way, oxaliplatin exhibits its anticancer activities. Compared with cisplatin and carboplatin, oxaliplatin displays a better tolerability but still has a few side-effects (e.g. acute dysesthesias, cumulative peripheral distal neurotoxicity) which limit its usage and narrow its clinical use.[8, 9]

To reduce the toxicities of the platinum drugs, polymers were used as drug delivery carriers for protection from blood clearance and protein binding.[10-13] However, at the early stage, the polymer carriers were mainly focused on non-biodegradable polymers and hydrophilic polymers.[14] Among these, a series of biodegradable poly(ethylene glycol)-b-poly(glutamic acid) platinum complexes were developed by Kataoka and coworkers.[11, 12] Although poly(ethylene glycol)-block-poly(glutamic acid) is biodegradable and water soluble(hydrophilic), it can self assemble into micelles with the Pt atoms as the cross-linking points.[15, 16] The exceptional physic-chemical and biological properties of the cisplatin-loaded micelle indicate them as an outstanding delivery system for cisplatin complexes and a phase I clinical trial has recently been completed in the UK (NC-6004, Nanocarrier Co. Ltd, Japan).[17, 18]

We focus on biodegradable but amphiphilic polymers for platinum drug delivery.[19-22] These polymers have a number of unique properties and are widely used for drug delivery of other anticancer drugs. Firstly, as biodegradable polymers, they are non-toxic and their degradation products can be assimilated or excreted under physiological conditions.[23] Secondly, as amphiphilic polymers, they can self-assemble into micelles and provide effective protection for the anticancer drugs.[24] Thirdly, these micelles can release the anticancer drugs under the intracellular condition of the cancerous cells;[25] and finally, they can be enriched in cancer tissues due to the enhanced permeation and retention (EPR) effect[26, 27] and thus do less harm to healthy cells or organs.

In our previous work,[20] poly(ethylene glycol)-block-poly(L-lactide co-2-methyl-2-allyloxycarbonylpropylene carbonate/ mercaptobutanedioic acid) (MPEG-b-P(LA-co-MAC/TMA)), a biodegradable amphiphilic block copolymer carrier, containing pendant 1,2-bidentate carboxyl groups was synthesized by thiol-ene radical addition and was used to chelate the active anticancer species (1,2-diamino-hexane-platinum, DACH-Pt) of

[a]Department of Obstetrics and Gynecology, Union Hospital, Tongji Medical College, Huazhong University of Science and Technology, Wuhan 430022, China,Tel: +86-2785351649. E-mail: zehuawang@163.net;
[b]State Key Laboratory of Polymer Physics and Chemistry, Changchun Institute of Applied Chemistry, Chinese Academy of Sciences, Changchun 130022, China;
[c] National Engineering Laboratory for Druggable Gene and Protein Screening, School of Life Science, Northeast Normal University, Changchun 130117, China, Tel: +86-431-89165937. E-mail: liwl100@nenu.edu.cn.
[†]These authors contributed equally to this work.
[*]Corresponding to prof. Zehua Wang and Wenliang Li PhD.

oxaliplatin to form mPEG-b-P(LA-co-MAC/TMA/DACH-Pt) complex, which can self-assemble into micelles with cytotoxicity against several cancer cells. It is worthy of mentioning here that the 1,2-dicarboxyl group can chelate with central Pt atom due to the formation of thermodynamically stable seven-membered ring. However, there is an extensive body of evidence implicating that increased level of cytoplasmic thiol-containing species such as glutathione (GSH) and thiol-containing proteins is a major cause of resistance to platinum drugs. Among them, notorious ones are the tripeptide glutathione and metallothioneins, which leads to platinum drug detoxification by sulfur binding.[28-31]Thus, a biodegradable amphiphilic polymer carrier, not only containing pendant 1,2-bidentate carboxyl groups, but also lacking potential hazardous sulfur to platinum is extremely desirable.

To develop this carrier, we focused on the block copolymers poly(ethylene glycol)-block-poly(L-lactideco-2-methyl-2-carboxyl-propylene carbonate) (MPEG-b-P(LA-co-MCC)) with pendant mono-carboxyl groups, which are used for EDC/NHS reaction with aspartic acid (ASP) to introduce pendant 1,2-dicarboxyl groups as a chelator for platinum atom. In this way, a biodegradable polymer-Pt(II) conjugate was successfully prepared. The self-assembly and in vitro antitumor efficacy on platinum resistant cancer cells were studied.

2 Experimental

2.1 Regents

The biodegradable drug carrier with pendant carboxyl groups, polyethylene glycol-poly(lactide-co-2-methyl-2-carboxyl-propylene carbonate) MPEG-b-P(LA-co-MCC) , was synthesized as previously described.[20, 22] The molecular formula of the polymer used in this paper was $MPEG_{5000}$-b-$P(LA_{1000}$-co-$MCC_{960})$ by proton nuclear magnetic resonance (^1H NMR). N-hydroxysuccinimide (NHS), 1-(3-dimethylaminopropyl)-3-ethylcarbodiimide hydrochloride (EDC·HCl), 3-(4,5-dimethylthiazol-2-yl)-2,5-diphenyltetrazolium bromide (MTT) and sodium azide were purchased from Sigma-Aldrich (Shanghai, China). Cisplatin (purity 99%) was bought from Shandong Boyuan Pharmaceutical Co. Ltd. (Shandong, China). All other chemicals and solvent were used as received.

2.2 General Methods

Inductively coupled plasma optical emission spectrometer (ICP-OES, iCAP 6300, Thermo scientific, USA) was used to determine the total platinum contents in the polymer-Pt conjugate and samples obtained outside of the dialysis bags in drug release experiments. Inductively coupled plasma mass spectrometer (ICP-MS, Xseries II, Thermo scientific, USA) was used for quantitative determination of trace levels of platinum. The morphology of the polymer micelles was measured on a JEOL JEM-1011 electron microscope. Particle size and zeta potential measurements were conducted on a Malvern Zetasizer Nano ZS90.

2.3 Preparation of the DACHPt aqueous complex

DACH-Pt aqueous complex were synthesized as previously described[20, 32] (Scheme 1). Briefly, $DACHPtCl_2$ was suspended in distilled water and mixed with silver nitrate (molar ratio: $AgNO_3$/$DACHPtCl_2$=2:1) to form an aqueous complex. The solution was kept in the dark at 25°C for 24 h, AgCl precipitates found after the reaction were eliminated by centrifugation, Afterward, the supernatant was purified by passage through a filter to get a DACH-Pt aqueous solution.

2.4 Synthesis of the 1,2-bidentate carboxyl groups functionalized carrier polymer MPEG-b-P(LA-co-MCC/ASP)

2 g MPEG-b-P(LA-co-MCC) (1.7 mmol caboxyl groups) was dissolved in 20 mL dry CH_2Cl_2 in a flask, to which DCC (0.7 g, 3.4 mmol), NHS (0.394 g, 3.4 mmol) and DMAP (0.122 g, 1 mmol) were added. The reaction mixture was kept under stirring in an ice bath for 24 h. Then it was filtered to remove the dicyclohexyl urea (DCU) formed and the filtrate was concentrated and precipitated by ethyl ether. The solid product was collected by filtration and dried under vacuum to obtain NHS ester MPEG-b-P(LA-co-MCC/NHS). Then this NHS ester (0.2 g, 0.16 mmol NHS group) was dissolved in dried water/DMF (1:1), followed by addition of aspartic acid (59 mg, 0.32 mmol). The reaction mixture was stirred at room temperature for 24 h and then it was dialyzed (Cutoff Mw 3500) against 2 L water for 1 day by changing water for 4 times. The product was first been frozen in a -80°C freezer overnight, and then was been moved to the VirTis AdVantage 2.0 Benchtop Freeze Dryer (SP Scientific, Gardiner, USA) for freeze drying for 2 days to obtain MPEG-b-P(LA-co-MCC/ASP) (0.18 g, yield 90%).

2.5 Preparation of the platinum loaded micelles

Platinum loaded micelles were prepared according to a previously described method,[20] MPEG-b-P(LA-co-MCC/ASP) was added into 20 mL secondary water and stirred for 30 minutes at room temperature, thereafter. Na_2CO_3 (30 mg) was added to the aqueous complex to neutralize the carboxyl groups. Then the DACHPt aqueous complex was added to the polymer solution, and the polymer-platinum complex was evacuated and purged with nitrogen and stirred vigorously for 24 h at 25 °C. After that, the MPEG-b-P(LA-co-MCC/ASP-Pt) complex solution was dialysised against the de-ionized water (Cutoff Mw 3500) for 12 h to remove the un-reacted platinum complex. The platinum loaded product, MPEG-b-P(LA-co-MCC/ASP-Pt) micelles, was abbreviated as “M(ASP-Pt)” hereafter.

2.6 Preparation of Rhodamine B-labelled copolymer (MPEG-b-P(LA-co-MCC/ASP-RhB))

The polymer MPEG-b-P(LA-co-MCC/ASP) was synthesized as described above. 0.2 g copolymer was dissolved in DMF (2 ml). Rhodamine B (10 mg) was added to the polymer solution. The mixture was kept stirred at room temperature for 24 h, followed by adding 6 ml water. The fluorescence-labeled copolymer MPEG-b-P(LA-co-MCC/ASP-RhB) was filtered by 0.2 μm membrane and dialyzed against 2 L water (dialysis bag

Cutoff Mw 3500) for 2 days. The micelles with Rhodamine B were lyophilized.

2.7 Preparation of fluorescence-labelled mixed micelles

1 mg of MPEG-b-P(LA-co-MCC/ASP-RhB) and 9 mg of M(ASP-Pt) complex were dissolved in 5 mL DMF in a 50 mL flask, and then 20 mL of deionized water was added to form mixed micelles. The micelle solution was freeze-dried for future use. The fluorescence-labeled mixed micelles were abbreviated as "M(RhB-Pt)" hereafter.

2.8 *In vitro* drug release profiles

Freeze-dried M(ASP-Pt) (50 mg) were dissolved in 25 mL of phosphate buffered solution (PBS), and release of Pt complex was conducted with a dialysis bag (Cutoff Mw 3500) against 135 mL of phosphate buffer solution (0.01 M PBS, PH 7.4) and acetate buffer solutions (pH 5.0) at 37 °C. The released Pt in the dialysis medium was measured by ICP-OES at pre-determined time intervals and the cumulative released Pt percentage was calculated and plotted against the drug release time.

2.9 Cell lines and cell culture

Human ovarian cancer cell line SKOV3 and the drug-resistant line SKOV3DDP cells were purchased from China Center for Type Culture Collection (Wuhan, China) and grown in RPMI 1640 (Gibco, Beijing, China) supplemented with 10% fetal bovine serum (Hyclone, Beijing) and 1% penicillin/streptomycin in 5% CO_2 at 37 °C. All the cells used in this project were within 30 passages since purchase.

2.10 Cytotoxicity of the M(ASP-Pt) micelles

The cytotoxicity test was conducted to evaluate *in vitro* antitumor activity of the M(ASP-Pt) by the MTT assay. SKOV3 and SKOV3DDP cells were chosen as a pair of sensitive and resistant ovarian cancer cells. Briefly, SKOV3 and SKOV3DDP cells harvested in a logarithmic growth phase were seeded in 96-well plates at a density of 5000 cells/well and incubated in RPMI-1640 for 12 h. The medium was then replaced with RPMI 1640 containing oxaliplatin and M(ASP-Pt) at a final equivalent Pt concentration from 0.1 to 100 μM. For each drug concentration, four replicates were set. The incubation time for all drugs was 48 h. After incubation, 20 μL of MTT solution in PBS with the concentration of 5 mg/mL was added and the plates were incubated for another 4 h at 37 °C, followed by removal of the culture medium containing MTT and addition of 150 μL of DMSO to each well to dissolve the formazan crystals formed. Finally, the plates were shaken for 10 minutes, and the absorbance of formazan product was measured at 492 nm by a microplate reader.

2.11 Cellular uptake

SKOV3 cells were grown in RPMI 1640 with 10% fetal bovine serum at 37 °C in 5% CO_2. The cells were seeded in 6-well plates and grown for 24 h prior to incubation with M(RhB-Pt) at 0.2 mg/mL. Live cells were imaged 6 h post-treatment using an inverted microscope (TE2000-U, Nikon). Pictures were taken with a digital camera (DXM1200F, Nikon). For quantitative examination, SKOV3 and SKOV3DDP cells were seeded at a density of 100×10^4 cells per well in 6-well plates, after exposure to 50 μM of oxaliplatin and M(ASP-Pt) for 2 h and 6 h, cells were washed by cold PBS three times and harvested by trypsin. The cells were counted and lysed by 70% HNO_3, evaporated to dry by heating, and then dissolved in 0.5 ml DI water. The Pt content was determined by ICP-MS. The uptake of drugs was expressed as "ng Pt per million cells".

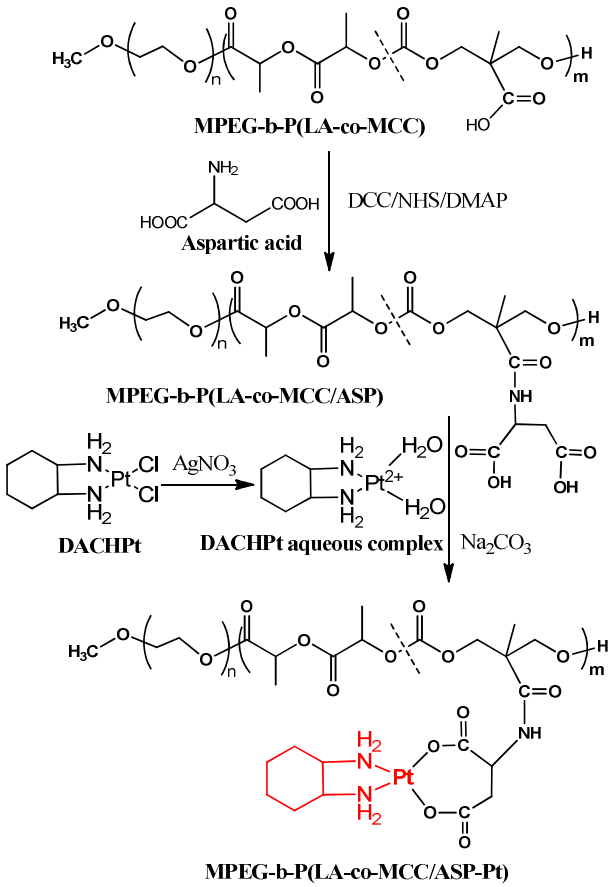

Scheme 1. Preparation of MPEG-b-P(LA-co-MCC/ASP-Pt) micelles.

3 Results and Discussion

3.1 Synthesis of the carrier polymer MPEG-b-P(LA-co-MCC/ASP)

Delivering of platinum(II) antitumor drugs to cancer cells has been a hot pursuit for decades.[10, 11, 13, 32-35] Because the carboxylate ligands are leaving groups, they are often replaced with polymeric carboxyl or dicarboxyl groups for chelating and delivering platinum(II) drugs.[3, 4] It is believed that the platinum antitumor species can be released, irrespective of the polymer backbone. In our previous work,[19, 20, 22] a biodegradable amphiphilic block copolymer carriers, MPEG-b-P(LA-co-MCC) was chosen as a starting material. This copolymer contained pendant carboxyl groups on its hydrophobic P(LA-co-MCC) segment, which was a random copolymer of L-lactide (LA) and 2-methyl-2-carboxyl-propylene carbonate (MCC). The reason for choosing this copolymer is the ease and high efficiency of MCC monomer synthesis, and the possibility to utilize the DCC/NHS reaction for the next step derivatization. In fact, the carboxyl groups were converted to 1,2-dicarboxyl groups by

reaction with aspartic acid (ASP) (Scheme 1). The reaction was carried out in two steps. First, the carboxyl group in the polymer chain was transformed to NHS ester; secondly, the NHS esters in the polymer chain were replaced by aspartic acid in water. After 24 h of reaction, the carboxyl groups were completely converted as evidenced by the ^{1}H NMR spectra. As shown in Figure 1B, the new peaks at δ= 4.45 and 2.77 assigned to the protons of methine and methylene in the 1,2-dicarboxyl groups of ASP backbone. Based on the ^{1}H NMR of spectra in Figure 1(A) and (B), the polymer compositions were calculated to be $MPEG_{5000}$-b-$P(LA_{1000}$-co-$MCC_{960})$ and $MPEG_{5000}$-b-$P(LA_{1000}$-co-$MCC_{960}/ASP_{800})$, respectively, where the subscripts denote block-number-average molecular weight M_n of PEG and total M_n of LA, MCC and ASP units. The molecular weight of ASP is 133.1. So, every polymer chain contains approximately six (800/133.1=6.01) ASP residues. Moreover, because there are ten LA and seven MCC units per parent polymer $MPEG_{5000}$-b-$P(LA_{1000}$-co-$MCC_{960})$, the DCC/NHS reaction efficiency is determined as ~86% (6/7=0.86).

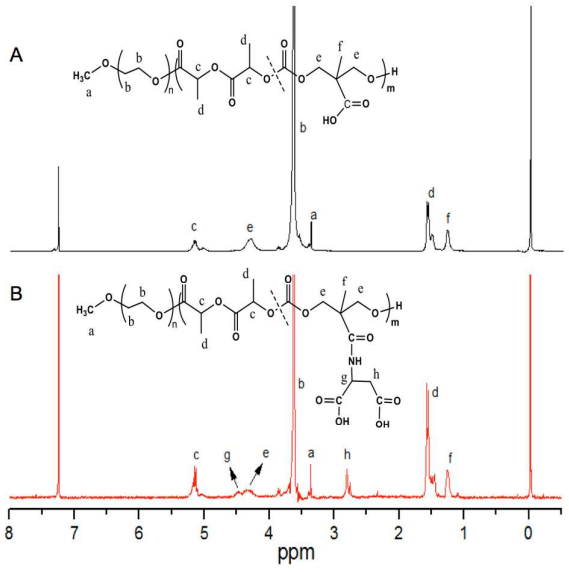

Figure 1. ^{1}H NMR spectra of (A) MPEG-b-P(LA-co-MCC) and (B) MPEG-b-P(LA-co-MCC/ASP) in $CDCl_3$.

3.2 Preparation of M(ASP-Pt) micelles

The M(ASP-Pt) micelles were prepared as shown in Scheme 1: (1) preparation of DACHPt aqueous complex by reacting DACH-Pt-Cl_2 with aqueous silver nitrate; (2) neutralization of the pendant 1,2-dicarboxyl groups by sodium carbonate; (3) mixing DACHPt aqueous complex with the polymer solution prepared in step 2; (4) dialyzing the micellar solution against the deionized water (Cutoff Mw 3500) for 12 h and lyophilizing it to a powder sample.

The amphiphilic nature of the polymer M(ASP-Pt) makes it possible to self-assemble into micelles with the P(LA-co-MCC/ASP-Pt) block as the inner core and the MPEG block as the hydrophilic shell.[20, 22, 33, 36, 37] Although both ASP and DACHPt aqueous complex are hydrophilic, the consuming of the free COOH groups on ASP, the formation of DACHPt-ASP complex during the chelation and the tractive force of hydrophobic block of the polymer makes DACHPt to come into the inner core of the micelles. Therefore, the DACHPt species buried in the polymer matrix would be protected effectively. Compared with MPEG-b-P(LA-co-MAC/TMA-Pt) micelles in our previous work, there were no sulfur atom exist for the M(ASP-Pt) M(ASP-Pt) micelles, which be desired to improve the antitumor efficiency.

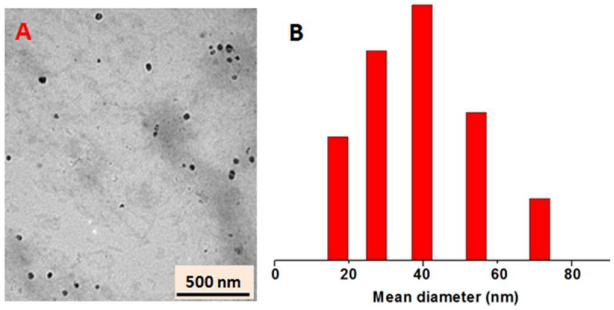

Figure 2. (A) TEM morphology and (B) DLS characterization of M(ASP-Pt) micelles.

3.3 Characterization of M(ASP-Pt) micelles

TEM and DLS were used to characterize the morphology and size of M(ASP-Pt) micelles. Typical TEM pictures are shown in Figure 2A. They had spherical structure with an average diameter of about 40-50 nm. DLS measurement (Figure 2B) showed that the micelles had a unimodal size distribution with an average diameter of 35-45 nm and a polydispersity index of 0.136, in agreement with those determined by TEM images.

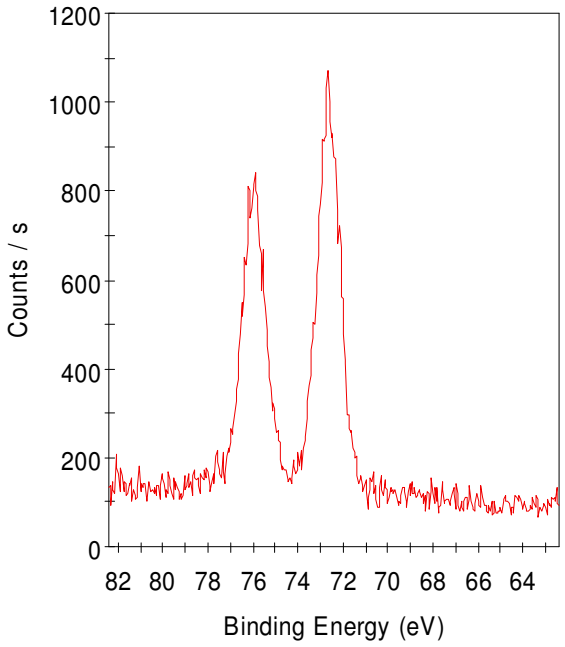

Figure 3. XPS curves of Pt_{4f} for M(ASP-Pt) micelles.

The zeta potential of M(ASP-Pt) micelles was measured. The results showed that it has an evident negative potential of -12.7mV, which is beneficial for circulation in blood.[38, 39]

It is vital to keep the oxidation state of Platinum in +2 valence in the preparation process and storage of M(ASP-Pt) micelles, because the anticancer activity is related to Pt(II) species. X-ray photoelectron spectroscopy (XPS) was used to characterize the oxidation state of Pt. As shown in figure 3, the binding energies determined for Pt_{4f} were 72.5 and 75.7 eV. They are identical to those of K_2PtCl_4 (73.2 and 76.4 of the 4f(7/2) and 4f(5/2) levels of Pt(II), respectively, and bigger than those of Pt black (71.0 and 74.5 eV of the 4f(7/2) and 4f(5/2) levels of Pt, respectively.[40] Therefore, it is deduced that the central Pt atoms in M(ASP-Pt) micelles are Pt(II).

3.4 Platinum content in the M(ASP-Pt) micelles

The Platinum content of the M(ASP-Pt) micelles was 9.6% w/w by ICP-OES. The molecular formula of carrier polymer was $MPEG_{5000}$-b-P(LA_{1000}-co-MCC_{960}/ASP_{800}) and the molecular weight was ~7760. The molecular weight of DACHPt is 309. Suppose that x is the number of platinum atoms attached to a single polymer chain, we can write the equation:

$$\frac{195x}{309x+7760} = 9.6\%$$

X = 4.5 from the above equation. It means that there are 4.5 DACHPt residues in one polymer chain. As addressed above, there are approximately 6 ASP residues in every polymer chain. Correspondingly, the conjugation rate of ASP residues is 75% (4.5/6=0.75).

3.5 Drug release from M(ASP-Pt) micelles

Drug release experiments from the micelles were evaluated by dialysis method and performed in phosphate buffered saline (PBS, pH 7.4) and acetate buffer solutions (pH 5.0), respectively. ICP-OES was used to determine the amount of platinum released. Release of platinum was observed in sustained manner from the micelles. The weight ratio of accumulative released platinum to the total platinum payload in the micelles was measured as a function of release time.

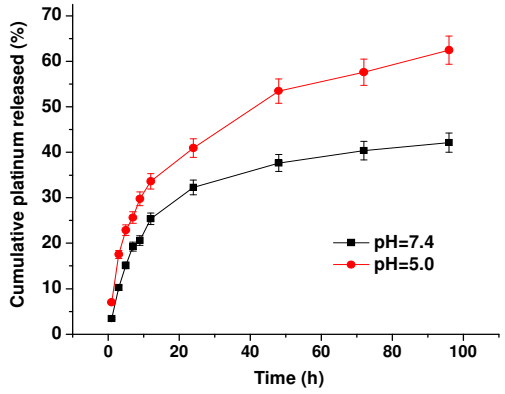

Figure 4. Drug release profiles of M(ASP-Pt) micelles at pH 5.0 and pH 7.4 buffered solution.

As shown in figure 4, the platinum rate from the micelles at pH 5.0 was significantly faster than that as pH 7.4. To release 50% of the total platinum payload took 41 h at pH 5.0, while it took more than 100 h at pH 7.4. This difference is attributed to the pH sensitivity of hydrolysis reaction of M(ASP-Pt) micelles. It is well known that both the ester bond in the polymer chains and the carboxylate-Pt chelated bond are more hydrolysable in more acidic solutions.

3.6 *In vitro* Cell viability studies

We show a representative dose-dependent cell viability curve of cisplatin for the human ovarian cancer cell line SKOV3 and the corresponding acquired resistant cell line SKOV3DDP (Fig. S1). SKOV3DDP shows a much more inert response to cisplatin, indicating the inability of cisplatin to kill the resistant cancer cells, which may be the major cause of clinical tumor recurrence. Our previous study has demonstrated that the MPEG-b-P(LA-co-MCC) polymer and polyesters with similar structures were nontoxic, hence the cytotoxicity observed here should be attributed to the released DACHPt. As we can see in Fig. 5A and Fig.5B, M(ASP-Pt) was as effective as cisplatin or oxaliplatin, both against SKOV3 and SKOV3DDP. The details were illustrated in Fig. 5C, the IC_{50} of cisplatin for SKOV3 and SKOV3DDP were 3.17 μM and 7.89 μM respectively, making a resistance fold of 2.5. Moreover, the IC_{50} values of oxaliplatin towards SKOV3 and SKOV3DDP were 3.87 μM and 8.31 μM respectively. The resistance fold is around 2.2. It seems that oxapliplatin is incapable to overcome the cisplatin resistance to a full extent. However, M(ASP-Pt) had IC_{50} values of 4.80 μM and 7.95 μM on SKOV3 and SKOV3DDP cells respectively, the resistance index was just 1.7 fold, indicating the SKOV3DDP was not as resistant to the nanoparticles as it was to cisplatin or oxaliplatin, in other words, the M(ASP-Pt) was able to overcome the drug resistance to some extend on ovarian cancer cells SKOV3DDP.

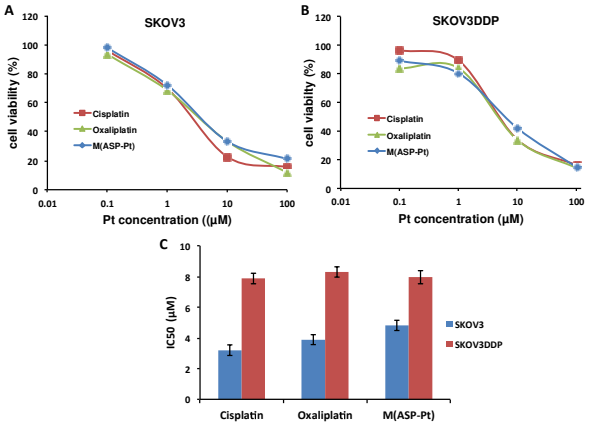

Figure 5. Representative dose dependent cell viability versus drug concentration curve of M(ASP-Pt) on cisplatin sensitive SKOV3 cells (A) and cisplatin resistant SKOV3DDP cells (B). Cisplatin and Oxaliplatin were used as two controls. The IC_{50} values were collected and shown (C). Data were shown as mean values ± standard deviation (n=3).

3.7 Cellular uptake of M(ASP-Pt)

To visually observe the nanoparticles internalized by cancer cells, we prepared fluorescence labeled ASP-Pt-loading nanoparticles, M(RhB-Pt), and observed the uptake by cancer cells. The Fig.6B showed the fluorescence within the SKOV3 cells, indicated that the cancer cells had effectively internalized the M(RhB-Pt) nanomicelles just as we expected. The high efficiency of cellular uptake could contribute to the way the internalization of nanoparticles by cancer cells. As we know, the nanoparticles get into cells via endocytosis while the free drugs by passive diffusion or the transporter pathway,[12, 41, 42] and the former way is much more efficient than the latter ones, as many literatures described.[42-44]

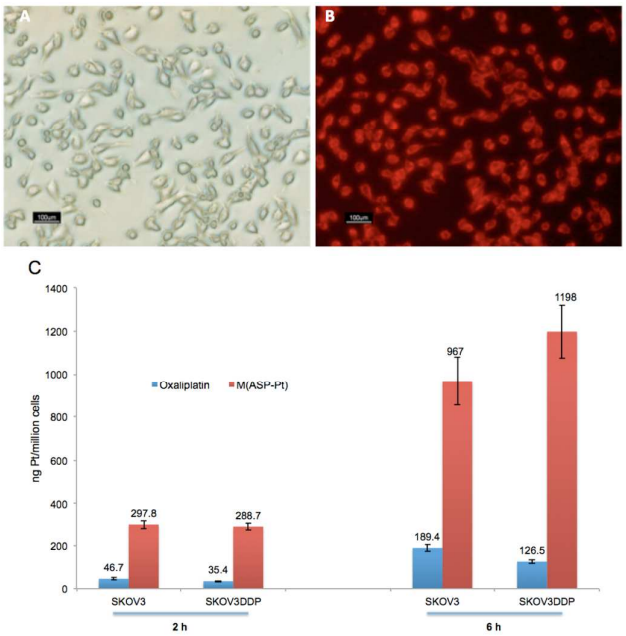

Figure 6. *In vitro* cellular uptake of RhB-labeled nanomicelles (A, B, red) and quantitative analysis of the uptake of oxaliplatin and M(ASP-Pt) (C).

To quantitative analyze the advantage of the M(ASP-Pt) nanomicelles, we also evaluated the intracellular platinum levels of cells exposed to oxaliplatin and M(ASP-Pt) for 2 h and 6 h. As we can see in Fig. 6c, after exposed to oxaliplatin, regardless of 2 h or 6 h, the platinum level of SKOV3DDP cells was lower than that of the parental SKOV3 cells. However, treated with the M(ASP-Pt), the platinum level within SKOV3DDP cells was as comparable as or even higher than that of SKOV3 cells. Take 6 h as an example, the levels of platinum within SKOV3 and SKOV3DDP treated with oxaliplatin were 189.4 ng Pt/million cells and 126.5 ng Pt/million cells, respectively, while the case of M(ASP-Pt) was 967 ng Pt/million cells *vs* 1198 ng Pt/million cells.

We can also conclude that with the same exposure time, the platinum levels of M(ASP-Pt) groups were much higher than those of oxaliplatin groups, both in SKOV3 cells and SKOV3DDP cells. For example, it was 1198 ng Pt/million cellswithin SKOV3DDP cells for 6 h exposure to M(ASP-Pt), while exposure to the same dosage of oxaliplatin could only get 126.5 ngPt/million cells into cells, almost 10-fold increase made by the nanomicelle approach. These gave a reasonable explanation to the low resistance fold we observed above and justified the strategy of M(ASP-Pt).

Taken together, we can say that by nanoparticle delivery, platinum drugs were internalized to the cancer cells to a greater extent, which helps to overcome platinum drug resistance. Meanwhile, it is well known that the EPR effect of solid tumor could significantly increase the accumulation of nano-scale substances within the tumor tissues,[10, 13] so there is a great chance that the *in vitro* results can translate to *in vivo* situation since the *in vivo* models can take advantage of both the EPR effect and the cell-level endocytosis.

Conclusions

In summary, we synthesized a biodegradable polymer carrier MPEG-b-P(LA-co-MCC/ASP), utilized the ASP residue to chelate with DACH-Pt and avoided the detoxification associated with disulfide bond since the ASP doesn't contain any sulfur atoms. The MPEG-b-P(LA-co-MCC/ASP-Pt) conjugate formed nanomicelles M(ASP-Pt) showed remarkable enhancement of intracellular drug accumulation and partially overcome drug resistance in ovarian cancer cells SKOV3DDP. It is worthy of further *in vivo* investigating and could be a promising approach to overcome the drug resistance problem.

Acknowledgements

This work was supported by the National Natural Science Foundation of China (81272860), by the Wuhan Science and Technology Bureau (2014060101010042), by the China Postdoctoral Science Foundation (2014M550163), and by the Research Funds from Science & Technology Department of Jilin Province (20140520049JH and 20130201008ZY).

References

1 F. Petrelli, A. Coinu, M. Ghilardi, M. Cabiddu, A. Zaniboni and S. Barni, *American journal of clinical oncology*, 2015, **38**, 227-233.
2 G. Zhang, X. P. Li, B. J. Liu, J. L. Wang, S. J. Wang, H. Cui and L. H. Wei, *Chinese medical journal*, 2013, **126**, 4477-4482.
3 G. Amr Ael, K. A. Ali and M. M. Abdalla, *European journal of medicinal chemistry*, 2009, **44**, 901-907.
4 E. Raymond, S. Faivre, J. M. Woynarowski and S. G. Chaney, *Seminars in oncology*, 1998, **25**, 4-12.
5 R. Yin, S. Gou, X. Liu and L. Lou, *Journal of inorganic biochemistry*, 2011, **105**, 1095-1101.
6 M. A. Graham, G. F. Lockwood, D. Greenslade, S. Brienza, M. Bayssas and E. Gamelin, *Clinical cancer research*, 2000, **6**, 1205-1218.
7 J. L. Misset, H. Bleiberg, W. Sutherland, M. Bekradda and E. Cvitkovic, *Critical reviews in oncology/hematology*, 2000, **35**, 75-93.
8 J. Cassidy and J. L. Misset, *Seminars in oncology*, 2002, **29**, 11-20.
9 N. V. Kolomeyevskaya, S. B. Lele, A. Miller, G. C. Riebandt, B. L. Blum, K. O. Odunsi and P. J. Frederick, *International journal of gynecological cancer*, 2015, **25**, 42-48.

10 K. J. Haxton and H. M. Burt, *Journal of pharmaceutical sciences*, 2009, **98**, 2299-2316.
11 N. Nishiyama, S. Okazaki, H. Cabral, M. Miyamoto, Y. Kato, Y. Sugiyama, K. Nishio, Y. Matsumura and K. Kataoka, *Cancer research*, 2003, **63**, 8977-8983.
12 N. Nishiyama, Y. Kato, Y. Sugiyama and K. Kataoka, *Pharmaceutical research*, 2001, **18**, 1035-1041.
13 R. H. Prabhu, V. B. Patravale and M. D. Joshi, *International journal of nanomedicine*, 2015, **10**, 1001-1018.
14 M. Kissel, P. Peschke, V. Subr, K. Ulbrich, A. M. Strunz, R. Kuhnlein, J. Debus and E. Friedrich, *European journal of nuclear medicine and molecular imaging*, 2002, **29**, 1055-1062.
15 B. Cao, S. Yan, K. Zhang, Z. Song, X. Chen, L. Cui and J. Yin, *Macromolecular bioscience*, 2011, **11**, 1211-1217.
16 J. J. Yoo, Y. I. Jeong, C. W. Chung and D. H. Kang, *Journal of nanoscience and nanotechnology*, 2014, **14**, 6256-6260.
17 K. Endo, T. Ueno, S. Kondo, N. Wakisaka, S. Murono, M. Ito, K. Kataoka, Y. Kato and T. Yoshizaki, *Cancer science*, 2013, **104**, 369-374.
18 R. Plummer, R. H. Wilson, H. Calvert, A. V. Boddy, M. Griffin, J. Sludden, M. J. Tilby, M. Eatock, D. G. Pearson, C. J. Ottley, Y. Matsumura, K. Kataoka and T. Nishiya, *British journal of cancer*, 2011, **104**, 593-598.
19 W. L. Li, W. J. Zhang, X. Y. Yang, Z. G. Xie and X. B. Jing, *J Appl Polym Sci*, 2014, **131**.
20 Q. Yang, H. H. Xiao, J. Cai, Z. G. Xie, Z. H. Wang and X. B. Jing, *Rsc Adv*, 2014, **4**, 61124-61132.
21 H. Xiao, D. Zhou, S. Liu, Y. Zheng, Y. Huang and X. Jing, *Acta biomaterialia*, 2012, **8**, 1859-1868.
22 H. Xiao, H. Song, Q. Yang, H. Cai, R. Qi, L. Yan, S. Liu, Y. Zheng, Y. Huang, T. Liu and X. Jing, *Biomaterials*, 2012, **33**, 6507-6519.
23 F. Rancan, U. Blume-Peytavi and A. Vogt, *Clinical, cosmetic and investigational dermatology*, 2014, **7**, 23-34.
24 Y. Wen and J. H. Collier, *Current opinion in immunology*, 2015, **35**, 73-79.
25 Y. Wen, H. R. Kolonich, K. M. Kruszewski, N. Giannoukakis, E. S. Gawalt and W. S. Meng, *Molecular pharmaceutics*, 2013, **10**, 1035-1044.
26 N. Bertrand, J. Wu, X. Xu, N. Kamaly and O. C. Farokhzad, *Advanced drug delivery reviews*, 2014, **66**, 2-25.
27 R. G. Qi, S. H. Wu, H. H. Xiao, L. S. Yan, W. L. Li, X. L. Hu, Y. B. Huang and X. B. Jing, *J Mater Chem*, 2012, **22**, 18915-18922.
28 D. J. Smith, M. Jaggi, W. Zhang, A. Galich, C. Du, S. P. Sterrett, L. M. Smith and K. C. Balaji, *Urology*, 2006, **67**, 1341-1347.
29 30.P. Borst, S. Rottenberg and J. Jonkers, *Cell cycle*, 2008, **7**, 1353-1359.
30 N. Eckstein, Journal of experimental & clinical cancer research: CR, 2011, **30**, 91.
31 M. Pasello, F. Michelacci, I. Scionti, C. M. Hattinger, M. Zuntini, A. M. Caccuri, K. Scotlandi, P. Picci and M. Serra, *Cancer research*, 2008, **68**, 6661-6668.
32 H. Cabral, N. Nishiyama, S. Okazaki, H. Koyama and K. Kataoka, *Journal of controlled release*, 2005, **101**, 223-232.
33 H. Xiao, H. Song, Y. Zhang, R. Qi, R. Wang, Z. Xie, Y. Huang, Y. Li, Y. Wu and X. Jing, *Biomaterials*, 2012, **33**, 8657-8669.
34 H. Uchino, Y. Matsumura, T. Negishi, F. Koizumi, T. Hayashi, T. Honda, N. Nishiyama, K. Kataoka, S. Naito and T. Kakizoe, *British journal of cancer*, 2005, **93**, 678-687.
35 Y. Mizumura, Y. Matsumura, T. Hamaguchi, N. Nishiyama, K. Kataoka, T. Kawaguchi, W. J. Hrushesky, F. Moriyasu and T. Kakizoe, *Japanese journal of cancer research: Gann*, 2001, **92**, 328-336.
36 Y. Wei, Y. X. Wang, W. Wang, S. V. Ho, F. Qi, G. H. Ma and Z. G. Su, *Langmuir*, 2012, **28**, 13984-13992.
37 E. C. Gryparis, M. Hatziapostolou, E. Papadimitriou and K. Avgoustakis, European journal of pharmaceutics and biopharmaceutics, 2007, **67**, 1-8.
38 A. N. Lukyanov, W. C. Hartner and V. P. Torchilin, Journal of controlled release, 2004, **94**, 187-193.
39 R. Wang, H. H. Xiao, H. Q. Song, Y. Zhang, X. L. Hu, Z. G. Xie, Y. B. Huang, X. B. Jing and Y. X. Li, *J Mater Chem*, 2012, **22**, 25453-25462.
40 B. Xing, H. Zhu, Y. Shi and W. Tang, Biometals, 2001, **14**, 51-57.
41 S. Y. Loh, P. Mistry, L. R. Kelland, G. Abel and K. R. Harrap, *British journal of cancer*, 1992, **66**, 1109-1115.
42 N. Oh and J. H. Park, *International journal of nanomedicine*, 2014, **9 Suppl 1**, 51-63.
43 A. C. Anselmo and S. Mitragotri, Journal of controlled release, 2014, **190**, 531-541.
44 M. S. Arayne and N. Sultana, *Pakistan journal of pharmaceutical sciences*, 2006, **19**, 258-268.